Available online at www.sciencedirect.com

ScienceDirect

Geochimica et Cosmochimica Acta 211 (2017) 341–354

Geochimica et Cosmochimica Acta

www.elsevier.com/locate/gca

Towards reconstructing ancient seawater Mg/Ca by combining porcelaneous and hyaline foraminiferal Mg/Ca-temperature calibrations

J.C. Wit [a], L.J. de Nooijer [b,*], J. Haig [a,1], F.J. Jorissen [c], E. Thomas [d,e], G.-J. Reichart [b,a]

[a] *Department of Geochemistry, Utrecht University, Utrecht 3508 TA, The Netherlands*
[b] *Department of Ocean Systems, NIOZ-Royal Netherlands Institute for Sea Research and Utrecht University, Den Burg, Netherlands*
[c] *UNAM Université, Université d'Angers, UMR CNRS 6112 LPGN-BIAF – Laboratory of Recent and Fossil Bio-Indicators. 2, Boulevard Lavoisier, 49045 Angers Cedex, France*
[d] *Department of Geology and Geophysics, Yale University, New Haven, CT 06520-8109, USA*
[e] *Department of Earth and Environmental Sciences, Wesleyan University, Middletown, CT 06459, USA*

Received 27 February 2012; accepted in revised form 28 May 2017; available online 16 June 2017

Abstract

The temperature of the deep ocean plays a vital role in the Earth's climate system. Paleo-reconstructions of deep-sea temperatures have traditionally been based on the oxygen isotope composition of deep-sea benthic foraminiferal calcite shells, although this parameter depends upon polar ice volume as well as temperature. More recent reconstructions use Mg/Ca in these shells, with temperature calibrations based on empirical relationships observed in present-day oceans. Incorporation of Mg (D_{Mg}) into foraminiferal calcite is, however, not solely dependent on temperature, but also on seawater Mg/Ca. Due to its long oceanic residence time, Mg concentrations remained relatively constant over time scales of a few hundred thousand years, but varied significantly over longer geological time scales. Accurate reconstruction of past temperatures using foraminiferal Mg/Ca, therefore, hinges on our understanding of Mg/Ca seawater changes on geological timescales. We explore a novel, independent approach to reconstructing past seawater Mg/Ca using the temperature-dependent offset in D_{Mg} between porcelaneous (secreting intermediate- or high-Mg calcite, abbreviated as IMC or HMC, respectively) and hyaline (producing low-Mg calcite, abbreviated as LMC) benthic foraminifera. We calibrated the Mg/Ca-temperature dependence for *Pyrgo* spp. (one of the few common, large-sized porcelaneous taxa present in the deep-sea since the middle Miocene), and combined this with an existing calibration of hyaline *Cibicidoides* spp. to mathematically solve for changes in Mg/Ca seawater through time. We show that changes in Mg/Ca seawater can be reconstructed using the offset between porcelaneous and hyaline foraminifera, but absolute values are highly dependent on the species-specific offset between Mg/Ca seawater and Mg-partition coefficients.

Keywords: Mg/Ca seawater; Benthic foraminifera; Temperature reconstructions; Proxy calibration

1. INTRODUCTION

Benthic foraminiferal Mg/Ca is a well-established proxy for reconstructing the temperature of the deep ocean, albeit influenced by the carbonate saturation state of deep waters

* Corresponding author.
E-mail address: ldenooijer@nioz.nl (L.J. de Nooijer).
[1] Present address: School of Earth and Environmental Sciences, James Cook University, Cairns, QLD 4870, Australia.

http://dx.doi.org/10.1016/j.gca.2017.05.036
0016-7037/

(Rosenthal et al., 1997; Lear et al., 2000, 2002; Martin et al., 2002; Rathmann et al., 2004; Elderfield et al., 2006; Yu and Elderfield, 2008). The application of Mg/Ca of foraminiferal calcite as a temperature proxy is based on temperature-dependent changes in the empirical partition coefficient D, which equals the ratio between Mg/Ca in the shell and that of these ions in seawater. Magnesium incorporation into test calcite (D_{Mg}) is, therefore, not only a function of temperature, but also depends on seawater Mg/Ca (e.g. Evans et al., 2015). The elemental composition of the ocean is controlled by a balance between the input of elements by rivers and the output due to carbonate and evaporite precipitation and through exchange of ions in hydrothermal flow during seafloor spreading (e.g. Dickson, 2002, 2004; Holland, 2005). Magnesium input into the oceans is primarily controlled by carbonate and silicate weathering, whereas output depends on the mole for mole exchange of Mg for Ca in hydrothermal flows and via dolomite formation (Hardie, 1996; Holland and Zimmerman, 2000; Holland, 2005). Removal of Mg from seawater through biomineralization is rather limited, whereas for Ca this is the most important pathway of removal from seawater.

The oceanic residence times, defined as the total amount of the element present in the global ocean divided by the removal or supply rate, are 1.1 Myr and 13 Myr for Ca and Mg respectively (Broecker and Peng, 1982). This implies that the modern ratio of Mg and Ca in seawater (5.2) may have varied on time scales of more than a million years (Wilkinson and Algeo, 1989). The ratio does not vary geographically or bathymetrically, because these residence times are much longer than the oceanic mixing time (approximately 1000 years).

If the Mg/Ca paleo-temperature proxy is to be applied on longer geological time scales, we thus need to correct for the Mg/Ca of seawater. Reliable temperature reconstructions are fundamental to our understanding of for instance, the evolution and magnitude of the cryosphere. Previous studies accounted for past changes in seawater Mg/Ca by applying low-resolution geochemical models (Lear et al., 2000, 2002, 2015; Billups and Schrag, 2002; Stanley et al., 2002) based on our understanding of Mg^{2+} and Ca^{2+} fluxes into and out of the modern oceans, and records of oceanic crustal cycling and dolomite abundance (Wilkinson and Algeo, 1989; Stanley and Hardie, 1998). Although these processes are well understood, rates are probably highly variable. Geochemical models of a higher resolution indeed show that variability in Mg/Ca seawater was underestimated (Fantle and DePaolo, 2006; Farkaš et al., 2007), which has a direct and significant impact on Mg/Ca based temperature reconstructions (Medina-Elizalde et al., 2008; Medina-Elizalde and Lea, 2010). The models have been constrained mainly by data on fluid inclusions in halite and calcium carbonate veins in ocean ridge flank basalts, recording past seawater Mg/Ca with a low temporal resolution (Lowenstein et al., 2001; Horita et al., 2002; Coggon et al., 2010). Such inclusions represent snapshots of ocean chemistry through time, allowing for a reconstruction of Mg/Ca seawater history over long time scales, but precluding a more continuous reconstruction.

We explore a novel approach for reconstructing seawater Mg/Ca by combining calcite Mg/Ca of porcelaneous and hyaline foraminifera. Interspecific differences in sensitivities in Mg-incorporation as a function of both seawater Mg/Ca and temperature can be used to constrain these two factors responsible for fossil foraminiferal Mg/Ca. Hyaline foraminifera produce shells with numerous pores that dominantly consist of low-Mg calcite (LMC; Erez, 2003). Porcelaneous foraminifera produce shells without pores consisting of Intermediate-Magnesium calcite or High-Magnesium Calcite (IMC or HMC, respectively), and use a different calcification mechanism (Debenay et al., 1998; Erez, 2003; Bentov and Erez, 2006; De Nooijer et al., 2009). The different wall types have contrasting relationships of Mg/Ca to temperature due to the dissimilar calcification mechanisms (Toyofuku et al., 2000; Erez, 2003; Bentov and Erez, 2006). Such species-specific responses to environmental parameters can be used to disentangle different parameters influencing calcite Mg/Ca. An example of this principle is given here by combining hyaline and porcelaneous Mg/Ca-temperature calibrations, allowing a more adequeate evaluation of Mg/Ca seawater through time.

The potential use of porcelaneous *Pyrgo* species as a paleo-temperature proxy has been demonstrated over a small (1–3 °C) (Healey et al., 2008), but not over a larger temperature gradient. First, we present a Mg/Ca-temperature calibration using the species *Pyrgo depressa* and *Pyrgo murrhina* from core tops. This calibration is then combined with a modified calibration for hyaline *Cibicidoides* species (Elderfield et al., 2006), allowing the development of an independent proxy for past seawater Mg/Ca. Secondly, the potential of this proxy is tested on a low-resolution Mg/Ca record for the last 10 Myr from the Walvis Ridge (southeastern Atlantic Ocean).

2. MATERIALS AND METHODS

Core top samples were taken with a classic Barnett multi-tube corer along a transect in the Bay of Biscay (Barnett et al., 1984) (Table 1), a semi-enclosed basin with a well-developed stratification due to the occurrence of water masses with rather constant temperature and salinity (Table 2) (Ogawa and Tauzin, 1973; Fontanier et al., 2002), creating an ideal environment for a Mg/Ca-temperature calibration (Reichart et al., 2003). Ambient bottom water temperature was maintained during recovery using an insulation device and measurements were done in duplicate within 30 min after core recovery. Sediments were stored in 500cm^3 bottles, with 95% ethanol and containing 1.0 g/l rose Bengal stain. In the laboratory, samples were gently shaken for several minutes in order to obtain a homogenous mixture, then sieved through 63 and 150 μm mesh screens (Fontanier et al., 2002). Samples were picked for rose Bengal-stained specimens of the porcelaneous benthic foraminifera *Pyrgo depressa* and *P. murrhina*.

Upper Miocene-Pleistocene *Pyrgo* and *Cibicidoides* species (*C. wuellerstorfi* and *C. mundulus*) were obtained from cores collected during Ocean Drilling Program (ODP) Leg 208 (Zachos et al., 2004) at Site 1264, at a water depth of 2507 m, near the crest of a North–South trending segment

Table 1
Depth, site temperature, size, Mg/Ca and Mn/Ca value of the used *Pyrgo* specimens for the Mg/Ca-temperature calibration based on samples from the Bay of Biscay. Mg/Ca and Mn/Ca values are averaged over 3–4 ablation craters per individual foraminifer. Uncertainties in Mg/Ca and Mn/Ca are based on the standard error of the average ($\sigma/\sqrt{n}$) and depend on the standard deviation and number of ablation profiles.

Depth (m)	Temperature (°C)	Size (μm)	Mg/Ca (mmol/mol)	Mn/Ca (mmol/mol)
550	10.80	1203	50.12 ± 1.10	0.32 ± 0.011
550	10.80	634	33.21 ± 1.91	0.30 ± 0.004
550	10.80	1431	49.87 ± 0.80	0.41 ± 0.020
550	10.80	650	40.74 ± 1.25	0.26 ± 0.002
1000	9.50	1041	33.91 ± 0.82	0.15 ± 0.002
1000	9.50	976	42.03 ± 3.25	0.18 ± 0.021
1000	9.50	1528	27.44 ± 1.23	0.24 ± 0.011
1000	9.50	520	17.39 ± 0.77	0.23 ± 0.007
1195	8.50	520	17.48 ± 0.30	0.03 ± 0.003
1264	8.75	911	14.46 ± 0.96	0.14 ± 0.009
1264	8.75	878	15.19 ± 1.92	0.15 ± 0.010
2000	3.85	683	18.55 ± 0.48	0.17 ± 0.010
2005	3.40	846	9.77 ± 0.46	0.05 ± 0.008
2800	2.60	618	12.43 ± 0.85	0.16 ± 0.008
2800	2.60	618	9.45 ± 0.28	0.26 ± 0.002
2850	3.27	585	12.78 ± 0.24	0.13 ± 0.020
4800	2.38	488	7.05 ± 0.42	0.13 ± 0.007
4800	2.38	390	8.90 ± 1.07	0.06 ± 0.005

Table 2
Depth, temperature and salinity of the different water masses in the Bay of Biscay after Ogawa and Tauzin (1973), Fontanier et al. (2002) and Fontanier et al. (2005).

Water mass	Depth	Temperature	Salinity
NACW[a]	150–800	11.9	35.60
MOW[b]	800–1200	10.5	35.80
IAW-PAW[c]	1200–3000	4.0	35.00
AABW[d]	3000–5000	3.0	34.95

[a] North Atlantic Central Water.
[b] Mediterranean Outflow Water.
[c] Intermediate Atlantic Water and Polar Atlantic Water (both North Atlantic Deep Water masses).
[d] Antarctic Bottom Water.

of the Walvis Ridge in the southeastern Atlantic Ocean. Sample depths are converted to the appropriate age using the shipboard age model (Zachos et al., 2004), based on magneto- and biostratigraphic datum levels, with the geomagnetic polarity time scale of Lourens et al. (2004).

Sample preparation for elemental analysis followed standard laboratory procedures (Barker et al., 2003). Samples were individually rinsed and sonically agitated 8 times with ultra pure water (6 times with 200 μl) and methanol (2 times with 200 μl) to remove any contamination caused by adhered detrital particles, then treated for 5 min with a buffered 1% H_2O_2 solution (200 μl) to remove any organic contaminants. No acid leach cleaning steps were used for *Pyrgo* spp., as their porcelaneous IMC shells are highly susceptible to dissolution, and *Cibicidoides* spp. to maintain a uniform cleaning procedure.

Elemental concentrations were measured on one or more chambers per individual with laser ablation inductively coupled mass spectrometry (LA-ICP-MS), measuring ^{24}Mg, ^{26}Mg, ^{27}Al, ^{42}Ca, ^{43}Ca, ^{44}Ca, ^{55}Mn, ^{88}Sr and their relative natural abundances. Ablation took place with a deep-ultraviolet-wavelength laser (193 nm) using a Lambda Physik Excimer laser system with GeoLas 200Q optics at a pulse repetition of 6 Hz for approximately 60 s with an energy density of 1.0 J/cm^2 (Reichart et al., 2003). A He-gas flow transported the ablated material, which was mixed with Argon prior to injection into the plasma of the quadrapole ICP-MS instrument (Micromass Platform ICP). Elemental concentrations were calculated from raw counts using computer software (Glitter). Elemental ratios with respect to Ca were based on the average of each ablation profile (Fig. 1). Element/Ca ratios of individual foraminifera were determined by averaging the values of 3–4 ablation profiles per single test. Although element/Ca profiles show variability through individual foraminiferal shells, there is no statistical difference between elemental concentrations measured on an in-house calcite standard by LA-ICP-MS and solution based ICP-OES, attesting to the quality of the element/ratio measurements on foraminiferal tests by LA-ICP-MS (Table 3).

Measurements are calibrated against the US National Institute of Standards and Technology SRM N610 glass (4.0 J/cm^2) and an in-house calcite standard GJR (1.0 J/cm^2) with Ca as an internal standard. Within this range, changing energy density between standard and sample does not affect the quantification of the element analyzed (Wit et al., 2010). Measurements were carefully checked for contamination by evaluating both Al and Mn of all individual test wall profiles. Contamination still adhering to the foraminiferal calcite despite the cleaning steps is identified by high Al concentrations in clay particles, whereas post depositional inorganic overgrowth was recognized through high Mn concentrations at the start of the ablation of the foraminiferal test. Since both phases potentially have high Mg concentrations compared to the test wall, these contaminants might also bias Mg measurements. All measured

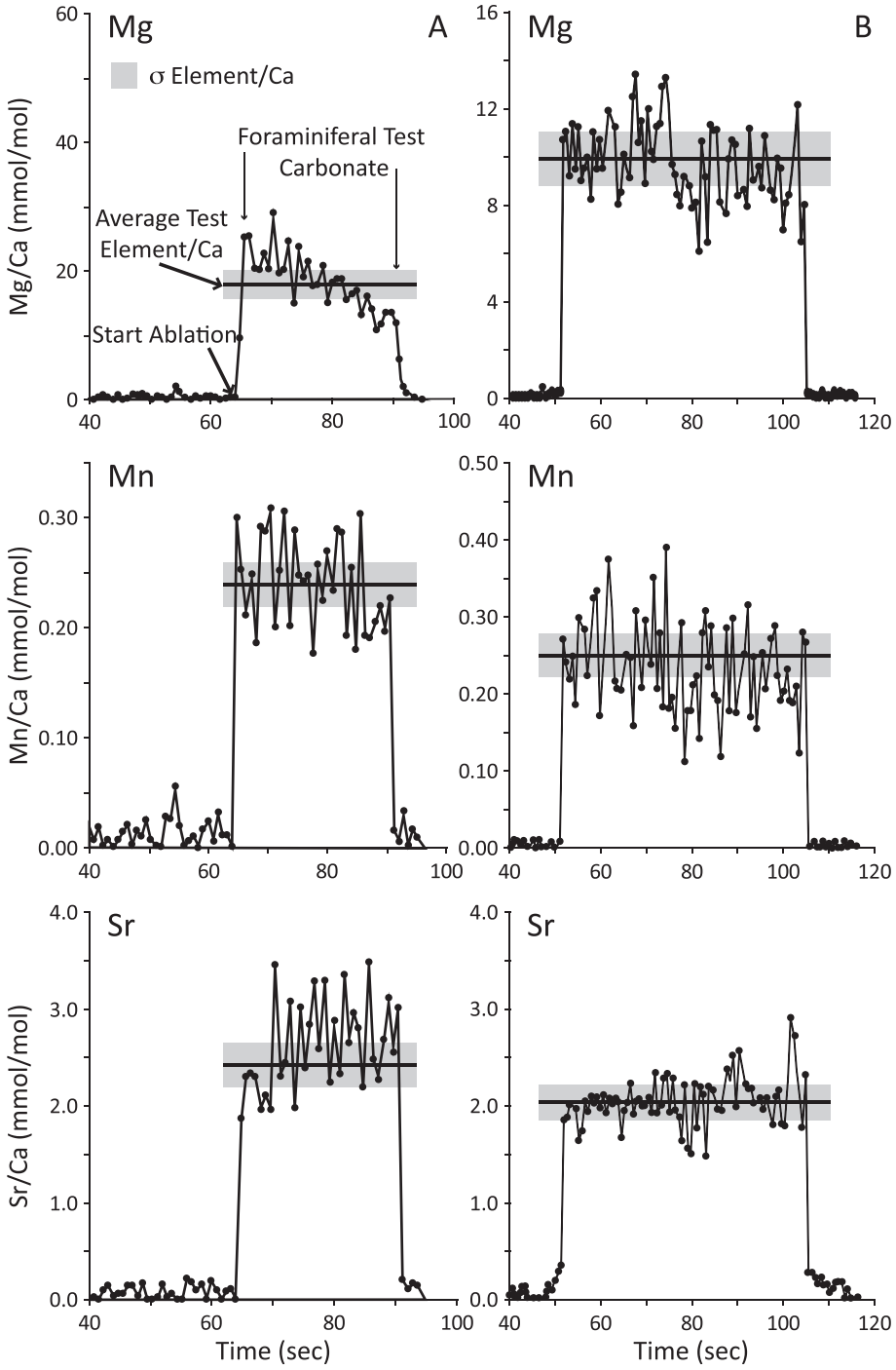

Fig. 1. Laser Ablation Mg/Ca, Mn/Ca and Sr/Ca profiles through the test of two *Pyrgo* specimens. The *Pyrgo* specimen A was retrieved from a sediment depth of 0–0.25 cm and a water depth of 1000 m, *Pyrgo* specimen B was retrieved from Sample 1264A 12H of the Walvis Ridge and has an age of 9.24 Ma. The absence of Mn/Ca peaks at the start and end of each ablation indicates that Mn is incorporated in the foraminiferal test carbonate during test wall formation and does not result from post mortem overgrowth.

calcite Mg/Ca from *C. mundulus* was species normalized to *C. wuellerstorfi* using a 0.16 mmol/mol correction, based on the average difference between both species as measured at Site 1264 (Naafs et al., 2008). This correction is comparable to the averaged difference of 0.28 mmol/mol between both species (Lear et al., 2000).

3. RESULTS

Magnesium/calcium values measured on *Pyrgo* spp. ranged from 7.1 to 50 mmol/mol (Fig. 2). Samples used for the *Pyrgo* spp. based temperature calibration from the Bay of Biscay represent a temperature gradient from ~2.4–11 °C

Table 3
Comparison between laser ablation (LA-ICP-MS) and solution (ICP-OES) based element data in ppm for in-house GJR calcite standard (Wit et al., 2010). Solution based data consists of three measurements of the in-house calcite standard, while the laser ablation data is derived from the 4 year average of the in-house standard during laser ablation ICP-MS measurements of foraminiferal calcite.

ICP-OES	Mg	Mn	Sr
Average	663	99	173
Standard deviation	35	0.40	4.3
Standard deviation (%)	5.2	0.41	2.5
N	3	3	3
LA-ICP-MS	Mg	Mn	Sr
Average	674	106	184
Standard deviation	61	7.2	15
Standard deviation (%)	9.1	6.9	8.0
N (4 year average)	643	643	643
Ratio	1.016	1.068	1.068

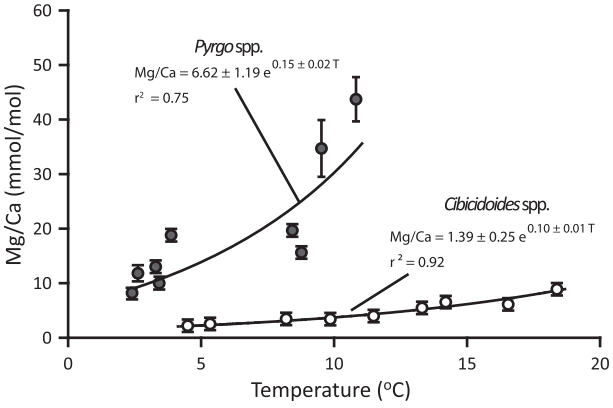

Fig. 2. Mg/Ca-temperature calibration for *Pyrgo* spp. from the Bay of Biscay (dark circles) and global *Cibicidoides* spp. (light circles). The data for *Cibicidoides* spp. is from Elderfield et al. (2006). *Pyrgo* spp. Error bars plotted for individual Mg/Ca values for *Pyrgo* spp. are based on the standard error of the mean ($\sigma/\sqrt{n}$). Regression lines and errors are calculated using the individual measurements. Uncertainties in the calibration (Eq. (1)) are calculated for the 95% confidence limits. The two individual *Pyrgo* spp. at 8.75 °C, may well have calcified at colder temperatures as they lived at the mixing depth of MOW and IAW (Table 2), as might be indicated by the relatively low Mg/Ca values.

(Table 1). Individual *Pyrgo* specimens show an increase in Mg/Ca with increasing temperatures. The regression line between bottom water temperatures and calcite Mg/Ca is represented by Eq. (1) ($r^2 = 0.75$, $p < 0.01$).

$$Mg/Ca = 6.62 \pm 1.19e^{(0.15\pm0.022*T)} \quad (1)$$

Furthermore, we see a positive correlation between size and Mg/Ca ($r^2 = 0.59$, $p < 0.01$), and a positive correlation between size and temperature, indicating that individual *Pyrgo* spp. are larger at higher temperatures ($r^2 = 0.42$, $p < 0.05$) (Table 4). A multiple regression using the equation $Mg/Ca_{pyrgo} = a^*e^{b*T} + c^*$ size showed that the impact of size and temperature are relatively independent, and that

Table 4
Pearson correlation coefficients and probability (p-value), indicating whether the Pearson correlation coefficients can be caused by chance alone, for *Pyrgo* from the Bay of Biscay.

Pearson coefficient	Size	Temperature
Size		0.423
Temperature	0.423	
Mg/Ca	0.589	0.782
Mn/Ca	0.525	0.545
Probability	Size	Temperature
Size		0.036
Temperature	0.036	
Mg/Ca	0.008	0.000
Mn/Ca	0.021	0.016

the effect of temperature is relatively large compared to that of the average foraminiferal size over the ranges studied here. The resulting regression is described by: $Mg/Ca_{pyrgo} = 0.0034 \quad (\pm 0.013) * e^{0.83(\pm 0.36)*T} + 0.019 \quad (\pm 0.0030) * Size$, where T is temperature in ^{0}C and size is the foraminiferal diameter in μm. All reported uncertainties are standard error of the means. It should be noted that such (potential) size-related effects on calcite chemistry are often ignored or uninvestigated in culturing studies. It remains to be investigated what the underlying effect of size on element partitioning might be (i.e. whether related to metabolism, microenvironmental changes and/or calcite precipitation rate).

Mn/Ca varied between 0.037 and 0.41 mmol/mol. The Mn was not present in coatings adhering to the outside of the test (Fig. 1), except for a few specimens. These were recognized as peak Mn values at the start of ablation, and subsequently excluded from the signal, before determining Mn/Ca values. Measured values for individual specimens of *Pyrgo* spp. co-vary positively with size ($r^2 = 0.53$, $p < 0.05$) and temperature ($r^2 = 0.55$, $p < 0.05$) (Table 4). Sr/Ca varied between 1.9 and 2.6 mmol/mol for *Pyrgo*.

Mg/Ca in upper Miocene-Recent *Cibicidoides* spp. and *Pyrgo* spp. from Site 1264 (Walvis Ridge) vary between 1.1 and 1.6 mmol/mol, and 7.0 and 10 mmol/mol respectively. The Mg/Ca values for *Cibicidoides* spp. and *Pyrgo* spp. do not clearly increase over time. Mg/Ca of both records do not co-vary ($r^2 = 0.04$, $p > 0.10$), implying that both changes in seawater Mg/Ca and temperature are changing over the interval studied (Fig. 3).

4. DISCUSSION

4.1. *Pyrgo* spp. based Mg/Ca temperature calibration

The *Pyrgo* spp. based temperature calibration shows a 15% change in Mg/Ca per °C temperature change (Fig. 2). Calibrations for the HMC foraminifer *Planoglabratella opercularis* and *Quinqueloculina yabei* (Toyofuku et al., 2000) have a much weaker steep slope (2–3%), which may be related to the difference in absolute Mg concentrations (approximately 10 times higher than in *Pyrgo* spp.). The Mg/Ca of these latter two foraminiferal species are

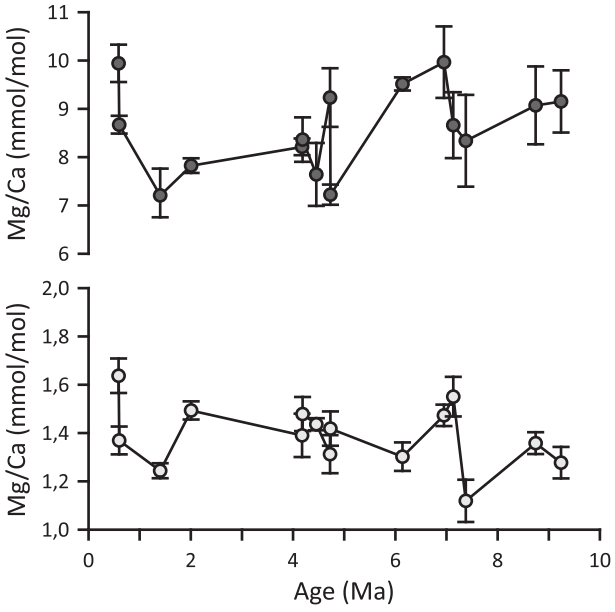

Fig. 3. Mg/Ca values of *Pyrgo* (dark) and *Cibicidoides* (light) specimens from ODP Leg 208 Site 1264. Error bars are based on the standard error of the mean ($\sigma/\sqrt{n}$).

of the same order of magnitude as those obtained from inorganic precipitation experiments (Ries, 2004). Results from these inorganic precipitation experiments potentially represent the maximum amount of Mg incorporation in seawater with the current seawater Mg/Ca without active biological fractionation against Mg. For the inorganic precipitation experiments, Mg/Ca increases with approximately 3% per °C (Ries, 2004), which is similar to those obtained for *P. opercularis* and *Q. yabei* (Toyofuku et al., 2000). A calibration of Mg incorporation in *Pyrgo murrhina* between 1.5–3.0 °C showed a steeper slope than Mg/Ca-temperature calibrations over a larger temperature gradient, with Mg/Ca increasing 57% per °C (Healey et al., 2008). Although the Mg/Ca are in the same range, the sensitivity reported by Healey et al. (2008) is steeper than the temperature sensitivity of 16% per °C of our study for that same temperature interval. The uncertainty in both calibrations are relatively large because of the relatively small temperature range (Healey et al., 2008) and limited number of measurements and relatively large inter-specimen variability (our results: Fig. 2). The here-reported uncertainty in the *Pyrgo*-calibration (Eq. (1), Fig. 2) is expected to decrease with an extended dataset. Existing temperature calibrations for the LMC, hyaline, perforate, benthic species *Oridorsalis umbonatus* and the genus *Cibicidoides* show a 8.6–10% change per °C (Rosenthal et al., 1997; Lear et al., 2002; Rathmann et al., 2004; Wit et al., 2012), which is somewhat lower than for the *Pyrgo* spp. calibration reported here.

The co-variation between test size and Mg/Ca suggests a potential ontogenetic effect (Table 4), which may impact the temperature calibration (Dueñas-Bohórquez et al., 2011) and should therefore be assessed before applying the Mg/Ca-temperature calibration of *Pyrgo* species down-core. Almost all coefficients for the correlations between size and the other parameters indicate that they are significant at the 0.01 or 0.05 level. Most coefficients are moderate (r^2 between 0.09–0.36), implying that variability in size can explain 9–36% of the total observed variability in Mg/Ca. The relative contribution of size to the observed variability within these parameters is thus limited, but present. Additionally, the size of measured *Pyrgo* spp. co-varies significantly with temperature (Table 4). We, therefore, argue that the relationship between Mg/Ca and size is not the result of an ontogenetic effect, but almost entirely results from co-variation with temperature, as was also argued for the benthic foraminifer *Ammonia tepida* (Wit et al., 2013). Since each sample consists of *Pyrgo* spp. specimens spanning a range of sizes, this variability with size is even less important when comparing averages.

To constrain the in-sediment depth habitat of the analyzed *Pyrgo*'s, we have analyzed test size and Mn/Ca. The positive correlation between the two suggests that larger *Pyrgo* spp. specimens live deeper in the sediment (Table 4), where they calcified under more elevated pore water Mn concentrations. *Pyrgo* species indeed have an infaunal carbon isotope signature (Magana et al., 2010), but have been observed to migrate vertically, from living epifaunally on the sediment surface to infaunally to depths of 3 cm (Linke and Lutze, 1993). Possibly, larger specimens spend, on average, more time deeper in the sediment. A more infaunal habitat preference at larger test size potentially introduces a carbonate ion effect on Mg incorporation (Elderfield et al., 2006). Bottom waters at the sampled sites are supersaturated with respect to calcite (Goyet et al., 2000), implying that $[CO_3^{2-}]$ most likely decreases within the pore water of the uppermost few cm of the sediment (Jourabchi et al., 2005; Elderfield et al., 2006). This potentially would lower the Mg concentrations of foraminiferal calcite (Elderfield et al., 2006; Dissard et al., 2010) of the larger specimens. The observed positive correlation between size and Mg/Ca indicates, however, that such a carbonate ion effect is probably insignificant or counter balanced by other effects. Since the overall impact of ontogeny, through whichever mechanism, is minor, it is ignored for our further discussion. Limiting the size range of analyzed specimens, as commonly is done for planktonic foraminifera, could improve future calibrations, although in practice the scarcity of specimens at greater water depths may prevent this. (see Table 5)

4.2. Reconstructing seawater Mg/Ca

The Mg/Ca-temperature calibration of porcelaneous *Pyrgo spp.* not only allows for the reconstruction of past temperatures but also introduces new possibilities. Combining the independent Mg/Ca to temperature calibrations for porcelaneous and hyaline foraminiferal species makes it possible to derive an equation for past seawater Mg/Ca. Calibrations of calcite Mg/Ca versus temperature are commonly expressed through an exponential relationship (Eq. (2)).

$$Mg/Ca_c = a \cdot e^{(b \cdot T)} \quad (2)$$

Table 5
Measured LA-ICP-MS Mg/Ca values with their standard deviations for fossil *Cibicidoides* spp. and *Pyrgo* spp. Standard deviations are based on 3–4 ablation profiles (Fig. 1) per individual. Average Mg/Ca values and standard error ($\sigma/\sqrt{n}$) for each depth are calculated with the unweighted average of the individual measurements of that depth.

Age (Ma)	Species	Mg/Ca (mmol/mol)	Average (mmol/mol)	$\sigma/\sqrt{n}$ (mmol/mol)
0.59	*Cibicidoides* spp.	1.43 ± 0.08		
0.59	*Cibicidoides* spp.	1.84 ± 0.05		
0.59	*Cibicidoides* spp.	1.71 ± 0.09		
0.59	*Cibicidoides* spp.	1.55 ± 0.03		
0.59	*Cibicidoides* spp.	1.43 ± 0.32		
0.59	*Cibicidoides* spp.	1.28 ± 0.22	1.54	0.08
0.60	*Cibicidoides* spp.	1.53 ± 0.14		
0.60	*Cibicidoides* spp.	1.21 ± 0.05	1.37	0.16
1.40	*Cibicidoides* spp.	1.25 ± 0.01		
1.40	*Cibicidoides* spp.	1.24 ± 0.12	1.24	0.01
2.01	*Cibicidoides* spp.	1.55 ± 0.03		
2.01	*Cibicidoides* spp.	1.46 ± 0.03		
2.01	*Cibicidoides* spp.	2.40 ± 0.09		
2.01	*Cibicidoides* spp.	0.99 ± 0.05		
2.01	*Cibicidoides* spp.	0.99 ± 0.05		
2.01	*Cibicidoides* spp.	1.47 ± 0.20	1.48	0.21
4.18	*Cibicidoides* spp.	1.33 ± 0.10		
4.18	*Cibicidoides* spp.	2.03 ± 0.05		
4.18	*Cibicidoides* spp.	1.37 ± 0.06		
4.18	*Cibicidoides* spp.	1.28 ± 0.09		
4.18	*Cibicidoides* spp.	0.93 ± 0.05	1.39	0.18
4.19	*Cibicidoides* spp.	1.70 ± 0.10		
4.19	*Cibicidoides* spp.	1.30 ± 0.05		
4.19	*Cibicidoides* spp.	1.19 ± 0.15		
4.19	*Cibicidoides* spp.	1.72 ± 0.29	1.48	0.14
4.46	*Cibicidoides* spp.	1.46 ± 0.09		
4.46	*Cibicidoides* spp.	1.22 ± 0.13		
4.46	*Cibicidoides* spp.	1.51 ± 0.34		
4.46	*Cibicidoides* spp.	1.51 ± 0.17		
4.46	*Cibicidoides* spp.	1.48 ± 0.29	1.44	0.05
4.72	*Cibicidoides* spp.	1.42 ± 0.02		
4.72	*Cibicidoides* spp.	1.21 ± 0.03	1.31	0.10
4.73	*Cibicidoides* spp.	1.45 ± 0.09		
4.73	*Cibicidoides* spp.	1.55 ± 0.11		
4.73	*Cibicidoides* spp.	0.98 ± 0.14		
4.73	*Cibicidoides* spp.	1.59 ± 0.05		
4.73	*Cibicidoides* spp.	1.52 ± 0.14	1.42	0.11
6.14	*Cibicidoides* spp.	1.17 ± 0.25		
6.14	*Cibicidoides* spp.	1.57 ± 0.05		
6.14	*Cibicidoides* spp.	1.17 ± 0.09	1.30	0.13
6.95	*Cibicidoides* spp.	1.16 ± 0.21		
6.95	*Cibicidoides* spp.	1.42 ± 0.17		
6.95	*Cibicidoides* spp.	1.81 ± 0.09		
6.95	*Cibicidoides* spp.	1.50 ± 0.03	1.47	0.13
7.14	*Cibicidoides* spp.	1.41 ± 0.17		
7.14	*Cibicidoides* spp.	1.37 ± 0.11		
7.14	*Cibicidoides* spp.	1.87 ± 0.13	1.55	0.16
7.38	*Cibicidoides* spp.	0.96 ± 0.09		
7.38	*Cibicidoides* spp.	1.28 ± 0.11	1.12	0.16
8.75	*Cibicidoides* spp.	1.50 ± 0.23		
8.75	*Cibicidoides* spp.	1.20 ± 0.12		
8.75	*Cibicidoides* spp.	1.21 ± 0.01		

(*continued on next page*)

Table 5 (*continued*)

Age (Ma)	Species	Mg/Ca (mmol/mol)	Average (mmol/mol)	$\sigma/\sqrt{n}$ (mmol/mol)
8.75	*Cibicidoides* spp.	1.39 ± 0.21		
8.75	*Cibicidoides* spp.	1.59 ± 0.13		
8.75	*Cibicidoides* spp.	1.25 ± 0.07	1.36	0.07
9.24	*Cibicidoides* spp.	1.55 ± 0.20		
9.24	*Cibicidoides* spp.	1.30 ± 0.27		
9.24	*Cibicidoides* spp.	1.30 ± 0.03		
9.24	*Cibicidoides* spp.	0.96 ± 0.19	1.28	0.12
0.59	*Pyrgo spp.*	9.66 ± 0.19		
0.59	*Pyrgo spp.*	10.60 ± 0.63		
0.59	*Pyrgo spp.*	9.56 ± 0.23	9.94	0.33
0.60	*Pyrgo spp.*	8.41 ± 0.51		
0.60	*Pyrgo spp.*	8.57 ± 0.40		
0.60	*Pyrgo spp.*	9.02 ± 0.16	8.67	0.18
1.40	*Pyrgo spp.*	7.73 ± 0.79		
1.40	*Pyrgo spp.*	6.74 ± 0.20		
1.40	*Pyrgo spp.*	6.18 ± 0.57		
1.40	*Pyrgo spp.*	8.17 ± 0.54	7.21	0.45
2.01	*Pyrgo spp.*	7.86 ± 0.22		
2.01	*Pyrgo spp.*	7.83 ± 0.44		
2.01	*Pyrgo spp.*	7.86 ± 0.57		
2.01	*Pyrgo spp.*	7.74 ± 0.17	7.82	0.03
4.18	*Pyrgo spp.*	7.99 ± 0.05		
4.18	*Pyrgo spp.*	8.55 ± 0.54		
4.18	*Pyrgo spp.*	8.09 ± 0.14	8.21	0.17
4.19	*Pyrgo spp.*	7.90 ± 0.02		
4.19	*Pyrgo spp.*	8.82 ± 0.58	8.36	0.46
4.46	*Pyrgo spp.*	8.93 ± 0.17		
4.46	*Pyrgo spp.*	7.11 ± 0.18		
4.46	*Pyrgo spp.*	6.87 ± 0.21	7.64	0.65
4.72	*Pyrgo spp.*	8.82 ± 0.77		
4.72	*Pyrgo spp.*	9.62 ± 0.42		
4.72	*Pyrgo spp.*	9.25 ± 0.45	9.23	0.23
4.73	*Pyrgo spp.*	7.50 ± 0.54		
4.73	*Pyrgo spp.*	7.63 ± 0.38		
4.73	*Pyrgo spp.*	6.73 ± 0.28		
4.73	*Pyrgo spp.*	7.02 ± 0.55	7.22	0.21
6.14	*Pyrgo spp.*	9.20 ± 0.31		
6.14	*Pyrgo spp.*	9.28 ± 0.15		
6.14	*Pyrgo spp.*	10.06 ± 0.32	9.51	0.27
6.95	*Pyrgo spp.*	10.70 ± 0.16		
6.95	*Pyrgo spp.*	9.22 ± 0.09	9.96	0.74
7.14	*Pyrgo spp.*	9.61 ± 0.23		
7.14	*Pyrgo spp.*	10.02 ± 0.19		
7.14	*Pyrgo spp.*	7.22 ± 0.17		
7.14	*Pyrgo spp.*	7.79 ± 0.11	8.66	0.68
7.38	*Pyrgo spp.*	6.92 ± 0.08		
7.38	*Pyrgo spp.*	6.68 ± 0.17		
7.38	*Pyrgo spp.*	9.04 ± 0.15		
7.38	*Pyrgo spp.*	10.70 ± 0.26	8.34	0.95
8.75	*Pyrgo spp.*	9.31 ± 0.32		
8.75	*Pyrgo spp.*	8.36 ± 0.15		
8.75	*Pyrgo spp.*	9.54 ± 0.09	9.07	0.36
9.24	*Pyrgo spp.*	7.66 ± 0.19		
9.24	*Pyrgo spp.*	9.90 ± 0.31		
9.24	*Pyrgo spp.*	9.89 ± 0.26	9.15	0.74

where T is the temperature in °C at the time of calcification, while $\boldsymbol{a}$ and $\boldsymbol{b}$ are empirically derived, species-specific, constants. Eq. (3) adds to this the ratio of seawater Mg/Ca at time T over the present day seawater Mg/Ca, and thus accounts for changes in seawater Mg/Ca over any geological time period.

$$\mathrm{Mg/Ca}_c = a \cdot \frac{\mathrm{Mg/Ca}_{present}}{\mathrm{Mg/Ca}_{past}} \cdot e^{(b \cdot T)} \quad (3)$$

Partitioning of Mg between seawater and calcite (D_{Mg}) depends not only on temperature, but is also affected by seawater Mg/Ca, especially in IMC- and HMC-producing species (Ries, 2004; Segev and Erez, 2006; Mewes et al., 2014). The linearity of this relationship (Eq. (3)) has indeed been questioned by a number of studies investigating the relationship between the Mg/Ca of the solutions and the partition coefficients. These authors suggested that a power relation would better fit the experimental data (Ries, 2004; Segev and Erez, 2006; Hasiuk and Lohmann, 2010; Raitzsch et al., 2010; Evans et al., 2015), and justify the introduction of a factor H to the relationship between Mg/Ca, Mg/Ca seawater and temperature (Eq. (4)).

$$\mathrm{Mg/Ca}_c = a \cdot \left(\frac{\mathrm{Mg/Ca}_{present}}{\mathrm{Mg/Ca}_{past}}\right)^{H} \cdot e^{(b \cdot T)} \quad (4)$$

The relationships between Mg/Ca, temperature and seawater Mg/Ca in both hyaline and porcelaneous foraminifera can now be expressed as two equations, in which T and $\mathrm{Mg/Ca}_{present}/\mathrm{Mg/Ca}_{past}$ are the respective products. It has so far implicitly been assumed that the shape of the calcite Mg/Ca – seawater Mg/Ca calibration is not affected by temperature (and vice versa). If this is the case, Eq. (5) can be used for the hyaline species, while Eq. (6) represents the porcelaneous species.

$$T = \frac{1}{b_h} LN\left(\frac{\mathrm{Mg/Ca}_h}{a_h \cdot \left(\frac{\mathrm{Mg/Ca}_{present}}{\mathrm{Mg/Ca}_{past}}\right)^{\mathrm{H}_h}}\right) \quad (5)$$

$$\left(\frac{\frac{\mathrm{Mg}}{\mathrm{Ca}\,present}}{\frac{\mathrm{Mg}}{\mathrm{Ca}\,past}}\right)^{\mathrm{H}_p} = (\mathrm{Mg/Ca}_p)/(a_p \cdot e^{(b_p \cdot T)}) \quad (6)$$

In which $\boldsymbol{a_h}$, $\boldsymbol{b_h}$ and $\boldsymbol{H_h}$ refer to the empirically derived constants for a hyaline species of foraminifera and $\boldsymbol{a_p}$, $\boldsymbol{b_p}$ and $\boldsymbol{H_p}$ to the constants for a porcelaneous foraminifera. Since, porcelaneous and hyaline taxa were picked from the same sample, they experienced identical T and $\mathrm{Mg/Ca}_{present}/\mathrm{Mg/Ca}_{past}$, so that Eq. (5) can be substituted into Eq. (6), resulting in Eq. (7).

$$\frac{\mathrm{Mg/Ca}_{present}}{\mathrm{Mg/Ca}_{past}} = \sqrt[\mathrm{H}_p - \mathrm{H}_h\left(\frac{b_p}{b_h}\right)]{\mathrm{Mg/Ca}_p \cdot a_p^{-1} \cdot \left(\frac{\mathrm{Mg/Ca}_h}{a_h}\right)^{\left(-\frac{b_p}{b_h}\right)}} \quad (7)$$

in which h refers to hyaline and p to porcelaneous foraminifera.

It should be noted that this exercise is equally applicable to any combination of species with a different Mg/Ca-temperature sensitivity and different absolute Mg/Ca. The combination of low-Mg hyaline and porcelaneous species has the advantage that these differences are relatively large and hence reduce the uncertainty in the reconstructed temperature and seawater Mg/Ca when compared to application of two species with more similar calibrations. The potential of Eq. (7) for reconstructing seawater Mg/Ca for the last 10 Myr was subsequently tested by analyzing Mg/Ca on the IMC porcelaneous *Pyrgo spp.* and the LMC precipitating hyaline *Cibicidoides spp.* from Walvis Ridge. Species-specific constants from the here presented Mg/Ca-temperature calibration for *Pyrgo* spp as well as from a modified Mg/Ca-temperature calibration (Elderfield et al., 2006) for *Cibicidoides* spp. were used to calculate Mg/Ca seawater. The calibration of Rosenthal et al. (1997) as revised by Lear et al. (2002) was modified because it generates unrealistically high temperatures at Walvis Ridge (Naafs et al., 2008). Therefore the sensitivity (exponential constant b) of the calibration was used, but the pre-exponential constant (a) was modified (from 1.36 to 1.18) to reflect accurate present day temperatures at Walvis Ridge (Naafs et al., 2008). The power relationship between seawater Mg/Ca and Mg/Ca is highly species specific, most likely varying between 0.4 and 1.0 (Evans and Müller, 2012; Evans et al., 2015). Fig. 4 shows the variability in seawater Mg/Ca as a result of the varying power relation (H varies between 0.4 and 1.0) for *Pyrgo* spp. and *Cibicidoides* spp., since the exact values are unknown for both species.

The exact value for H (Eq. (4)) is critical in estimating past seawater Mg/Ca and temperature (Figs. 4 and 5). From Eq. (7) it follows that reconstructed temperatures and past seawater Mg/Ca increase exponentially when values for $(H_p\text{-}H_h{}^{*}\ (b_p/b_h))$ approach 0. Therefore, culturing studies must constrain the species-specific values for H (as they have been for the constants a and b). Moreover, it should be tested whether H is constant over the range of reconstructed temperatures. As summarized by Evans and Müller (2012) and Evans et al. (2015), results from culturing studies indicated that a power function best describes the relationship between calcite Mg/Ca and seawater Mg/Ca (Delaney et al., 1985; Segev and Erez, 2006; Raitzsch et al., 2010). However, it remains to be determined which underlying mechanism is responsible for such a relationship, and why the seawater Mg/Ca – calcite Mg/Ca isn't equally well described by a linear function (see De Nooijer et al., accompanying paper). The reconstructions presented here (Figs. 4 and 5) indicate that despite the current uncertainties in the values for H_p and H_h, the combinations of $H_p = 0.6$ and $H_h = 0.4$ and $H_p = 0.8$ and $H_h = 0.6$ are unlikely, because they result in unrealistically high (i.e. >20 mol/mol) values for temperature and seawater Mg/Ca.

Reconstructed seawater Mg/Ca (both its absolute value as well as its trend in time) is very different according to the value for H in the power correction (H 0.4–1.0). Furthermore, other uncertainties are impinging on the reconstruction, mainly derived from four sources. Here we discuss the source of these uncertainties and their impact at a power correction of 0.4 (H_p) and 1.0 (H_h), keeping in mind that the impact and magnitude of these uncertainties also vary with varying H_p and H_h. The first uncertainty is caused by the used Mg/Ca-temperature calibration and its inherent uncertainty (95% confidence interval), as can be seen in

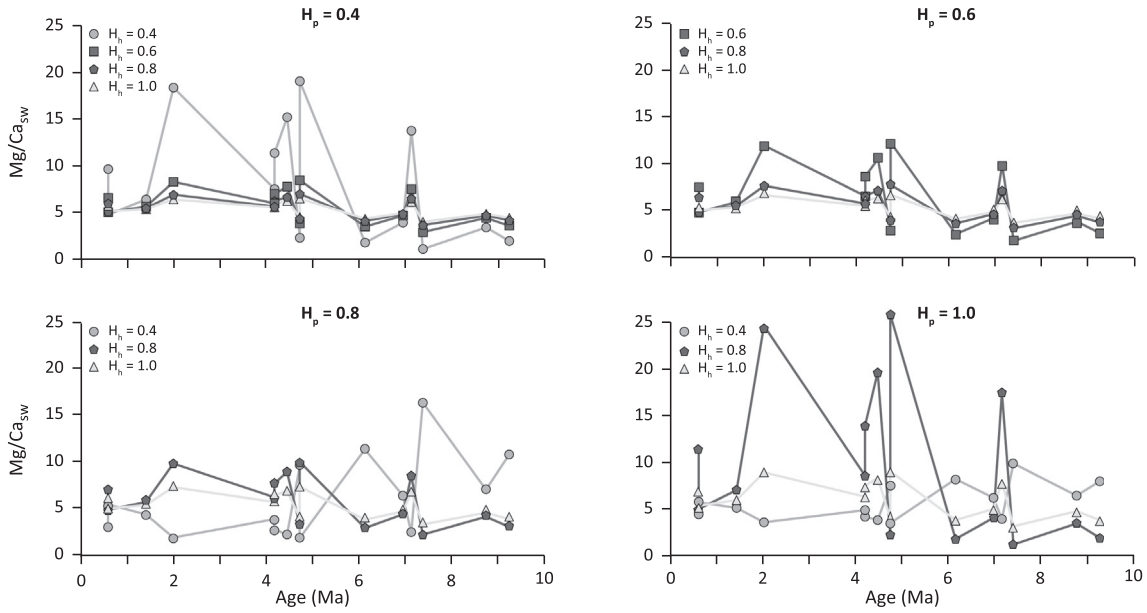

Fig. 4. Fluctuations in seawater Mg/Ca over the last 10 Ma derived from the Mg/Ca of *Pyrgo* spp. and *Cibicidoides* spp. based on Eq. (7). Values for seawater Mg/Ca are calculated using a power correction (R^H) for both *Pyrgo* spp. and *Cibicidoides* spp. varying between 0.4 and 1.0 (Evans and Müller, 2012). The four panels represent reconstructions based on four different values for H_p (0.4–1.0). Within every panel, up to four reconstructions are based on different values for H_h (0.4–1.0). Legend keys are given next to the axes on which seawater Mg/Ca is plotted. Reconstructions for the combinations $H_p = 0.6$/ $H_h = 0.4$ and $H_p = 0.8$/ $H_h = 0.6$ are not shown since they result in unrealistically high values for seawater Mg/Ca (e.g. >100 mol/mol).

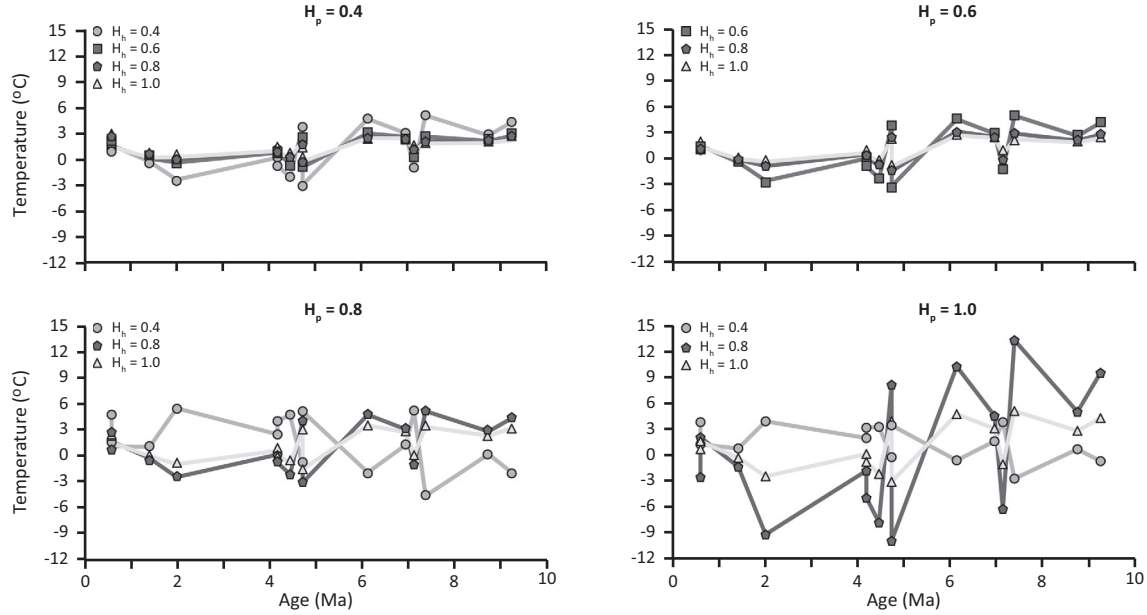

Fig. 5. Fluctuations in temperature independent of changes in seawater Mg/Ca over the last 10 Ma derived from the calcite Mg/Ca of *Pyrgo* spp. and *Cibicidoides* spp. based on Eq. (8). Temperature is calculated using the power correction (R^H) for both *Pyrgo* spp. and *Cibicidoides* spp. varying between 0.4 and 1.0 (Evans and Müller, 2012). The four panels represent reconstructions based on four different values for H_p (0.4–1.0). Within every panel, up to four reconstructions are based on different values for H_h (0.4–1.0). Legend keys are given next to the axes on which the temperature values are plotted. Reconstructions for the combinations $H_p = 0.6$/ $H_h = 0.4$ and $H_p = 0.8$/ $H_h = 0.6$ are not shown since they result in unrealistically high deep sea temperatures (>20 °C).

Eq. (1) and Fig. 2. These confidence intervals cause a maximum range of 7 mol/mol. The average uncertainty in seawater Mg/Ca as a result of uncertainties in Mg/Ca-temperature calibrations, expressed as a standard deviation, is 1–1.6 mol/mol. This uncertainty has, however, no effect on the reconstructed variability, as all points in the

reconstruction are affected equally by this factor. Reconstructed seawater Mg/Ca is most sensitive to changes in the porcelaneous Mg/Ca-temperature calibration. If future field- or experimental studies would change the calibrations applied here (Fig. 2), reconstructed past Mg/Ca would increase by higher values for both the pre-exponential and exponential constants. For example, Eq. (7) shows that a change in the exponential constant for the hyaline species (here *Cibicidoides* spp.) from 0.10 to 0.15 would increase the $Mg/Ca_{past}/Mg/Ca_{present}$ from 1.15 to 1.60, under average values for H_h and H_p and Mg/Ca_p and Mg/Ca_h and assuming that the pre-exponential constant remains the same.

The second uncertainty derives from the inter-individual variability when measuring Mg/Ca of fossil foraminifera (Fig. 3). The cause of this variability includes foraminiferal migration through the sediment during their lifetime, and it is not possible to quantify this for paleo-samples. Another component of this inter-individual variability is the variability between different species and morphotypes of the genus *Cibicidoides* (Rae et al., 2011). Although the exact contribution of each of these uncertainties to inter-individual variability is unknown, it is part of the inter-individual variability, generating an uncertainty in seawater Mg/Ca of 0.2–1.2 mol/mol.

The third uncertainty derives from the assumption that measured foraminifera lived at the same time and thus temperature. This assumption might, however, not be valid due to their different habitats and bioturbation, which could result in specimens recovered from the same depth having an offset in age of up to thousands of years. Millennial scale changes in temperature would then impact them differently. Still, temperature offsets will be relatively limited in deep-sea settings, such as that of the Walvis Ridge.

Finally, the potential impact of a carbonate ion effect on the Mg/Ca of *Pyrgo* spp. and *Cibicidoides* spp. needs to be assessed. *Pyrgo* spp. have a more infaunal depth habitat making them less susceptible to a potential carbonate ion effect (Linke and Lutze, 1993; Elderfield et al., 2006; Rathmann and Kuhnert, 2008; Magana et al., 2010). Mg/Ca for *Cibicidoides* spp., however, shows a small but significant carbonate ion effect, especially at bottom water temperatures below 4 °C (Elderfield et al., 2006; Yu and Elderfield, 2008). A carbonate ion effect on the here-reported Mg/Ca cannot be ruled out entirely, although we expect it to be minor, because Mg/Ca for *Pyrgo* spp. and *Cibicidoides* spp. are not significantly correlated (Fig. 3). Since a carbonate ion effect on the Mg/Ca of the *Cibicidoides* spp. cannot be ruled out, we calculated the effect on seawater Mg/Ca for a combination of H_p and H_h resulting in a seawater Mg/Ca reconstruction that relatively closely matches previously published ones (i.e. at H_p and H_h on 0.4 and 1.0). We assumed a 60 μmol/kg gradual increase in CO_3^{2-} concentration for the last 10 Ma (Zeebe, 2012). The sensitivity of foraminiferal Mg/Ca to changes in CO_3^{2-} for *Cibicidoides* spp. is 0.0086 mmol/mol for every μmol/kg change (Elderfield et al., 2006). The uncertainty in seawater Mg/Ca can be calculated using this sensitivity and the gradual increase in CO_3^{2-}, resulting in an uncertainty between 0.1–1.7 mol/mol, with an increasing uncertainty in the older samples. The sensitivity of 0.0086 is, however, determined using a global core-top data set, which might not reflect the sole impact of carbonate ion concentrations. Dueñas-Bohórquez et al. (2011b) calibrated a sensitivity for *Ammonia tepida* of 0.0012 mmol/mol per μmol/kg change in a culturing study. When this sensitivity is used to calculate the uncertainty in seawater Mg/Ca, it varies between 0.02–0.3 mol/mol.

Mg/Ca seawater shows an overall increase during the last 10 Myr, in spite of the high variability in Mg/Ca seawater associated with the changing values for the power correction (H) and the uncertainties associated described above (Fig. 4). For $H_p = 0.4$ and 0.6, seawater Mg/Ca increases from approximately 3 to 5 mol/mol, the exact value depending on the value for H_h (Fig. 4). With higher values used for H_p (0.8 or 1.0), the increase in seawater Mg/Ca is less clear and more variable between the different values for H_h. Furthermore, reconstructed Mg/Ca seawater values show large fluctuations on time scales shorter than, or similar to, the oceanic residence time of Mg and Ca respectively. The general increase seems to be in line with the increasing values for model based low-resolution Mg/Ca seawater curves, although they do not reflect the variability over shorter time scales (Wilkinson and Algeo, 1989; Hardie, 1996). A somewhat higher time-resolution model for the last 20 Myr based on a simplified geochemical model of the Ca cycle, combined with seawater Mg values derived from numerical models for diagenesis, with reaction rates determined by measuring the isotopic composition and concentration of Sr in pore waters, does show Mg/Ca seawater variability over these shorter time scales (Fantle and DePaolo, 2006).

We have shown that Mg/Ca seawater can be calculated when Eq. (5) is substituted into Eq. (6). This resulted in Eq. (7), which allows for the calculation of Mg/Ca seawater independent of temperature. Alternatively, Eq. (6) can be substituted into Eq. (5) (Eq. (8)), resulting in a Mg/Ca-temperature equation, which is theoretically independent of changes in Mg/Ca seawater, following the same lines of reasoning as demonstrated for Eq. (7).

$$T = \frac{LN \frac{Mg/Ca_h}{a_h \cdot ((Mg/Ca_p)/a_p)^{\frac{H_h}{H_p}}}}{b_h - \frac{H_h}{H_p} \cdot b_p} \quad (8)$$

Fig. 5 presents the reconstructed temperatures, free of variability in seawater Mg/Ca, for the last 10 Myr years with varying values for H_p and H_h. The large uncertainty in temperatures reconstructed from Eq. (8) indicates that the correction used for Mg/Ca seawater in Mg/Ca-based temperature reconstructions is vital, as demonstrated by the modeling approach of Medina-Elizalde et al. (2008, 2010), who showed a large underestimate of temperature compared to temperature reconstructions using the classic low resolution models (Lear et al., 2000; Billups and Schrag, 2002). Recognition of the changes in seawater Mg/Ca on shorter timescales is, therefore, of vital importance to reliably apply the Mg/Ca temperature proxy further back in geological time. However, the largest obstacle in using Mg/Ca seawater reconstructions to more accurately reconstruct Mg/Ca temperature is the form of

the correction itself, which depends on the power correction (H). Species-specific variability therein causes a large variability in seawater Mg/Ca (Fig. 4) and temperature (Fig. 5), as demonstrated here, and by the approach of Evans and Müller (2012) and Evans et al. (2015).

Although variable for the different combinations of Hp and Hh, most of the reconstructed trends in deep sea temperatures (Fig. 5) match previous reconstructions by showing a temperature decrease around ~5 Ma to present day. Depending on the assumed seawater Mg/Ca, combined $\delta^{18}O$ and Mg/Ca from benthic foraminifera showed a global decline in temperature from 5–6 to 0–2 °C (Cramer et al., 2011; Lear et al., 2000, 2002, 2010, 2015). These trends display a relatively gradual, long-term decrease in temperature, with overall less variability than presented here, although this may be partly explained by differences in temporal resolution. Another cause for the relatively smooth temperature decrease in previous studies is the assumed gradual change in seawater Mg/Ca over time, which is highly likely given the relatively long residence times of Ca^{2+} and Mg^{2+} in seawater (Broecker and Peng, 1982). Alternatively, an *a priori* gradual change in seawater Mg/Ca would imply that the values for H_p and H_h are most likely in the order of 0.4–0.6 and 0.6–1.0, respectively, since higher values for H_p and lower for H_h produce more variable reconstructions for bottom water temperature and seawater Mg/Ca.

5. CONCLUSIONS

The Mg/Ca in the tests of the porcelaneous foraminiferal genus *Pyrgo* records bottom water temperature. Combining this calibration with an existing calibration for *Cibicidoides* spp. and Mg/Ca values of this taxon in the same samples as used for measurements on *Pyrgo* potentially allows the deconvolution of Mg/Ca seawater. The use of species-specific responses to disentangle different parameters influencing a proxy is, therefore, a promising approach to further improve reconstructions of past climates. However, the unknown species-specific relationship between seawater Mg/Ca and D_{Mg} for *Pyrgo* spp. and *Cibicidoides* spp. hinders the current approach. Although the associated uncertainties in the current reconstruction effort are significant, this study shows that the currently used corrections for seawater Mg/Ca result in potentially large under- or overestimations in temperature reconstructions.

ACKNOWLEDGEMENTS

We would like to thank David Naafs for providing the necessary measurements needed for the correction between to *C. wuellerstorfi* and *C. mundulus*. We appreciate the assistance of Paul Mason, Helen de Waard and Gijs Nobbe with laser ablation analyses. The manuscript benefitted from the constructive comments of 3 anonymous reviewers, for which we are grateful. This research is funded by the Utrecht University and the Darwin Centre for Geobiology project "Biological validation of proxies for temperature, salinity, oxygenation and pCO_2 based on experimental evidence using benthic foraminiferal cultures" and US NSF OCE-1219948 grant to J.M Bernhard.

REFERENCES

Barker S., Greaves M. and Elderfield H. (2003) A study of cleaning procedures used for foraminiferal Mg/Ca paleothermometry. *Geochem. Geophys. Geosyst.* **4**, 8407.

Barnett P. R. O., Watson J. and Connely D. (1984) A multiple corer for taking virtually undisturbed sample from shelf, bathyal and abyssal sediments. *Oceanol. Acta* **7**, 399–408.

Bentov S. and Erez J. (2006) Impact of biomineralization processes on the Mg content of foraminiferal shells: a biological perspective. *Geochem., Geophys., Geosyst.* **7**, 11.

Billups K. and Schrag D. P. (2002) Paleotemperatures and ice volume of the past 27 Myr revisited with paired Mg/Ca and $^{18}O/^{16}O$ measurements on benthic foraminifera. *Paleoceanography* **17**, 11.

Broecker W. S. and Peng T.-H. (1982) *Tracers in the Sea*. Eldigo Press, Lamont-Doherty Geological Observatory, Palisades, New York, USA, p. 690.

Coggon R. M., Teagle D. A. H., Smith-Duque C. E., Alt J. C. and Cooper M. J. (2010) Reconstructing past seawater Mg/Ca and Sr/Ca from mid-ocean ridge flank calcium carbonate veins. *Science* **327**, 1114–1117.

Cramer B. S., Miller K. G., Barrett P. J. and Wright J. D. (2011) Late Cretaceous-Neogene trends in deep ocean temperature and continental ice volume: reconciling records of benthic foraminiferal geochemistry ($\delta^{18}O$ and Mg/Ca) with sea level history. *J. Geophys. Res. Oceans* **116**, C12023.

Debenay J. P., Guillou J. J., Geslin E., Lesourd M. and Redois F. (1998) Processus de cristallisation de plaquettes rhomboédriques à la surface d'un test porcelané de foraminifère actuel. *Geobios* **31**, 295–302.

Delaney M. L., Bé A. W. H. and Boyle E. A. (1985) Li, Sr, Mg, and Na in foraminiferal calcite shells from laboratory culture, sediment traps, and sediment cores. *Geochim. Cosmochim. Acta* **49**, 1327–1341.

De Nooijer L. J., Toyofuku T. and Kitazato H. (2009) Foraminifera promote calcification by elevating their intracellular pH. *PNAS* **106**, 15374–15378.

Dickson J. A. D. (2002) Fossil echinoderms as monitor of the Mg/Ca ratio of phanerozoic oceans. *Science* **298**, 1222–1224.

Dickson J. A. D. (2004) Echinoderm skeletal preservation: Calcite-Aragonite seas and the Mg/Ca ratio of phanerozoic oceans. *J. Sed. Res.* **74**, 355–365.

Dissard D., Nehrke G., Reichart G. J. and Bijma J. (2010) Impact of seawater pCO_2 on calcification and Mg/Ca and Sr/Ca ratios in benthic foraminifera calcite: results from culturing experiments with *Ammonia tepida*. *Biogeosciences* **7**, 81–93.

Dueñas-Bohórquez A., da Rocha R. E., Kuroyanagi A., De Nooijer L. J., Bijma J. and Reichart G. J. (2011a) Interindividual variability and ontogenetic effects on Mg and Sr incorporation in the planktonic foraminifer *Globigerinoides sacculifer*. *Geochim. Cosmochim. Acta* **75**, 520–532.

Dueñas-Bohórquez A., Raitzsch M., De Nooijer L. J. and Reichart G. J. (2011b) Independent impacts of calcium and carbonate ion concentration on Mg and Sr incorporation in cultured benthic foraminifera. *Marine Micropal.* **81**, 122–130.

Elderfield H., Yu J., Anand P., Kiefer T. and Nyland B. (2006) Calibrations for benthic foraminferal Mg/Ca paleothermometry and the carbonate ion hypothesis. *Earth Planet. Sci. Lett.* **250**, 633–649.

Erez J. (2003) The source of ions for biomineralization in foraminifera and their implications for paleoceanographic proxies. *Rev. Miner. Geochem.* **54**, 115–149.

Evans D. and Müller W. (2012) Deep time foraminifera Mg/Ca paleothermometry: nonlinear correction for secular change in seawater Mg/Ca. *Paleocanography* **27**, 1–11.

Evans D., Erez J., Oron S. and Müller W. (2015) Mg/Ca-temperature and seawater-test chemistry relationships in the shallow-dwelling large benthic foraminifera *Operculina ammonoides*. *Geochim. Cosmochim. Acta* **148**, 325–342.

Fantle M. S. and DePaolo D. J. (2006) Sr isotopes and pore fluid chemistry in carbonate sediment of the Ontong Java Plateau: Calcite recrystallization rates and evidence for a rapid rise in seawater Mg over the last 10 million years. *Geochim. Cosmochim. Acta* **70**, 3883–3904.

Farkaš J., Böhm F., Wallmann K., Blenkinsop J., Eisenhauer A., Van Geldern R., Munnecke A., Voigt S. and Vezier J. (2007) Calcium isotope record of Phanerozoic oceans: Implications for chemical evolution of seawater and its causative mechanisms. *Geochim. Cosmochim. Acta* **71**, 5117–5134.

Fontanier C., Jorissen F. J., Licari L., Alexandre A., Anschutz P. and Carbonel P. (2002) Live benthic foraminiferal faunas from the Bay of Biscay: faunal density, composition, and microhabitats. *Deep-Sea Res. I* **49**, 751–785.

Fontanier C., Jorissen F. J., Chaillou G., Anschutz P., Grémare A. and Griveaud C. (2005) Live foraminiferal faunas from a 2800 m deep lower canyon station from the Bay of Biscay: faunal response to focusing of refractory organic matter. *Deep-Sea Res. I* **52**, 1189–1227.

Goyet C., Healy R.J. and Ryan J.P., 2000. Global distribution of total inorganic carbon and total alkalinity below deepest winter mixed layer depths, ORNL/CDIAC-127, NDP-076.

Hardie L. A. (1996) Secular variation in seawater chemistry: an explanation for the coupled secular variation in the mineralogies of marine limestone and potash evaporites over the past 600 my. *Geology* **24**, 279–283.

Hasiuk F. J. and Lohmann K. C. (2010) Application of calcite Mg partitioning functions to the reconstruction of paleocean Mg/Ca. *Geochim. Cosmochim. Acta* **74**, 6751–6763.

Healey S. L., Thunell R. C. and Corliss B. H. (2008) The Mg/Ca-temperature relationship of benthic foraminiferal calcite: New core-top calibrations in the <4 °C temperature range. *Earth Planet. Sci. Lett.* **272**, 523–530.

Horita J., Zimmerman H. and Holland H. D. (2002) Chemical evolution of seawater during the Phanerozoic: implications from the record of marine evaporites. *Geochim. Cosmochim. Acta* **66**, 3733–3756.

Holland H. D. and Zimmerman H. (2000) The dolomite problem revisited. *Int. Geol. Rev.* **42**, 481–490.

Holland H. D. (2005) Sea level, sediments and the composition of seawater. *Americ. J. Sci.* **305**, 220–239.

Jourabchi P., Van Capellen P. and Regnier P. (2005) Quantitative interpretation of pH distributions in aquatic sediments: a reaction-transport modeling approach. *Am. J. Sci.* **305**, 919–956.

Lear C. H., Elderfield H. and Wilson P. A. (2000) Cenozoic Deep-Sea temperatures and Global ice volumes from Mg/Ca in benthic foraminiferal calcite. *Science* **287**, 269–272.

Lear C. H., Rosenthal Y. and Slowey N. (2002) Benthic foraminiferal Mg/Ca-paleothermometry: A revised core-top calibration. *Geochim. Cosmochim. Acta* **66**, 3375–3387.

Lear C. H., Mawbey E. M. and Rosenthal Y. (2010) Cenozoic benthic foraminiferal Mg/Ca and Li/Ca records: Toward unlocking temperatures and saturation states. *Paleoceanography* **25**, PA 4215.

Lear C. H., Coxall H. K., Foster G. L., Lunt D. J., Mawbey E. M., Rosenthal Y., Sosdian S. M., Thomas E. and Wilson P. A. (2015) Neogene ice volume and ocean temperatures: Insights from infaunal foraminiferal Mg/Ca paleothermometry. *Paleoceanography* **30**, 1437–1454.

Linke P. and Lutze G. F. (1993) Microhabitat preferences of benthic foraminifera – a static concept or a dynamic adaptation to optimize food acquisition? *Mar. Micropaleontol.* **20**, 215–234.

Lourens L. J., Hilgen F. J., Laskar J., Shackleton N. J. and Wilson D. (2004) The Neogene Period. In *A Geologic Time Scale 2 0 0 4* (eds. F. M. Gradstein, J. G. Ogg and A. G. Smith). Cambridge University Press, pp. 409–440.

Lowenstein T. K., Timofeff M. N., Brennan S. T., Hardie L. A. and Demicco D. V. (2001) Oscillations in phanerozoic seawater chemistry: evidence from fluid inclusions. *Science* **294**, 1086–1088.

Magana A. L., Southon J. R., Kennett J. P., Roark E. B., Sarnthein M. and Stott L. D. (2010) Resolving the cause of large differences between deglacial benthic foraminifera radiocarbon measurements in Santa Barbara Basin. *Paleoceanography* **115**.

Martin P. A., Lea D. W., Rosenthal Y., Shackleton N. J., Sarntheim M. and Papenfuss T. (2002) Quaternary deep sea temperature history derived from benthic foraminiferal Mg/Ca. *Earth Planet. Sci. Lett.* **198**, 193–209.

Medina-Elizalde M., Lea D. W. and Fantle M. S. (2008) Implications of seawater Mg/Ca variability for Plio-Pleistocene tropical climate reconstruction. *Earth Planet. Sci. Lett.* **3–4**, 585–595.

Medina-Elizalde M. and Lea D. W. (2010) Late Pliocene equatorial Pacific. *Paleoceanography* **25**, 10.

Mewes A., Langer G., De Nooijer L. J., Bijma J. and Reichart G. J. (2014) Effect of different seawater Mg^{2+} concentrations on calcification in two benthic foraminifers. *Marine Micropal.* **113**, 56–64.

Naafs B. D. A., Stap H. L., Thomas E., Lourens L., Reichart G. J. and Hodell D. A. (2008) Integrated oxygen isotope and Mg/Ca analysis of benthic foraminiferal species: the last 30 Myr. *Geophys. Res. Abstr.* **10**, EGU2008-A-10112.

Ogawa N. and Tauzin P. (1973) Contribution à l'étude hydrologique et géochimique du golfe de cap-breton. *Bulletin de l'institut Géologique du Bassin d'Aquitaine Bordeaux* **14**, 19–46.

Rae J. W. B., Foster G. L., Schmidt D. N. and Elliot T. (2011) Boron isotopes and B/Ca in benthic foraminifera: Proxies for the deep ocean carbonate system. *Earth Planet. Sci. Let.* **302**, 403–413.

Raitzsch M., Dueñas-Bohórquez A., Reichart G.-J., de Nooijer L. J. and Bickert T. (2010) Incorporation of Mg and Sr in calcite of cultured benthic foraminifera: impact of calcium concentration and associated calcite saturation state. *Biogeosciences* **7**, 869–881.

Rathmann S., Hess S., Kuhnert H. and Mulitza S. (2004) Mg/Ca ratios of the benthic foraminifera *Oridoralis umbonatus* obtained by laser ablation from core top sediments: Relationship to bottom water temperature. *Geochem. Geophys. Geosyst.* **5**, 10.

Rathmann S. and Kuhnert H. (2008) Carbonate ion effect on Mg/Ca, Sr/Ca and stable isotopes on the benthic foraminifera *Oridorsalis umbonatus* off Namibia. *Mar. Micropaleontol.* **66**, 120–133.

Reichart G.-J., Jorissen F., Anschutz P. and Mason P. R. D. (2003) Single foraminiferal test chemistry records the marine environment. *Geology* **31**, 355–358.

Ries J. B. (2004) Effect of ambient Mg/Ca ratio on Mg fractionation in calcareous marine invertebrates: A record of the oceanic Mg/Ca ratio over the Phanerozoic. *Geology* **32**, 981–984.

Rosenthal Y., Boyle E. A. and Slowey N. (1997) Temperature control on the incorporation of magnesium, strontium, fluorine, and cadmium into benthic foraminiferal shells from Little Bahama Bank: prospects for thermocline paleoceanography. *Geochim. Cosmochim. Acta* **61**, 3633–3643.

Segev E. and Erez J. (2006) Effect of Mg/Ca ratio in seawater on shell composition in shallow benthic foraminifera. *Geochem. Geophys. Geosyst.* **7**, 8.

Stanley S. M. and Hardie L. A. (1998) Secular oscillations in the carbonate mineralogy of reef-building and sediment-producing organisms driven by tectonically forced shifts in seawater chemistry. *Palaeogeogr. Palaeoclimatol. Palaeoecol.* **144**, 3–19.

Stanley S. M., Ries J. B. and Hardie L. A. (2002) From the Cover: Low-magnesium calcite produced by coralline algae in seawater of Late Cretaceous composition. *PNAS* **99**(24), 15323–15326.

Toyofuku T., Kitazato H., Kawahata H., Tsuchiya M. and Nohara M. (2000) Evaluation of Mg/Ca thermometry in foraminifera: Comparison of experimental results and measurements in nature. *Paleoceanography* **15**, 456–464.

Wilkinson B. H. and Algeo T. J. (1989) Sedimentary carbonate record of calcium-magnesium cycling. *Americ. J. Sci.* **289**, 1158–1194.

Wit J. C., Reichart G.-J., Jung S. J. A. and Kroon D. (2010) Approaches to unravel seasonality in sea surface temperatures using paired single specimen foraminiferal $\delta^{18}O$ and Mg/Ca analyses. *Paleoceanography* **25**, 1–15.

Wit J. C., De Nooijer L. J., Barras C., Jorissen F. J. and Reichart G. J. (2012) A reappraisal of the vital effect in benthic foraminifera on Mg/Ca values: species specific uncertainty relationships. *Biogeosciences* **9**, 3693–3704.

Wit J. C., De Nooijer L. J., Wolthers M. and Reichart G. J. (2013) A novel salinity proxy based on Na incorporation into foraminiferal calcite. *Biogeosciences* **10**, 6375–6387.

Yu J. and Elderfield H. (2008) Mg/Ca in the benthic foraminifera *Cibicidoides wuellerstorfi* and *Cibicidoides mundulus*: temperature versus carbonate ion saturation. *Earth Planet. Sci. Lett.* **276**, 129–139.

Zachos J. C., Kroon D. and Blum P. (2004) Initial Reports Leg 208. *Proc. Ocean Dril. Prog.* **208**, 73.

Zeebe R. E. (2012) History of seawater carbonate chemistry, atmospheric CO_2, and ocean acidification. *Annu. Rev. Earth Planet. Sci.* **40**, 141–165.

Associate editor: Thomas M. Marchitto